

# Manufacturing and Characterization of Physically Modified Aluminum Anodes Based Air Battery with Electrolyte Circulation

Jaewook Lee<sup>1,3</sup>, Changyong Yim<sup>1</sup>, Deug Woo Lee<sup>2</sup>, and Simon S. Park<sup>1,#</sup>

<sup>1</sup> Department of Mechanical and Manufacturing Engineering, Schulich School of Engineering, University of Calgary, 2500 University Dr. N.W. Calgary, Alberta, T2N 1N4, Canada

<sup>2</sup> Department of Nanomechatronics Engineering, Pusan National University, 2, Busandaehak-ro 63beon-gil, Geumjeong-gu, Busan, 46241, South Korea

<sup>3</sup> Research Institute of Green Science and Technology, Shizuoka University, 836 Ohya, Suruga, Shizuoka, 4228017, Japan

# Corresponding Author | Email: simon.park@ucalgary.ca, TEL: +1-403-220-6959, FAX: +1-403-282-8406

KEYWORDS: Aluminum-Air battery, Anode surface modification, Micro-Sandblasting, Electrolyte circulation

*Recently, the aluminum–air (Al–air) battery has spotlighted since its low cost, sustainable properties, and high theoretical potential. To improve battery performance, several approaches for Al anode modification have been introduced, such as alloy processes, metal oxide deposition, etc. However, such processes could induce critical side effects during battery operation for example, by-product creation by de-alloying, reduction of Al activity, and more. In this research, to overcome these problems, physically modified Al foils were used as Al anodes and an Al–air battery was fabricated. The Al anode was sandblasted by micro-sand blasting, employing around 10  $\mu\text{m}$  beads, to increase surface area and reactivity. Indeed, an electrolyte solution was circulated between the battery structures to enhance cell stability and remove by-products from the anode reaction. The energy capacity of air battery with the sandblasted Al anode was 3.85 mWh and it was about 5 times improved than that of bare Al anode case. In addition, the energy capacity in the electrolyte circulation case was 4.5 mWh, which established that battery performance was increased about 6.5 times by the sandblasting and electrolyte circulation process. Therefore, this new type of Al–air battery has a great potential to be applied in various fields.*

Manuscript Received: May 19, 2016 | Revised: August 23, 2016 | Accepted: September 27, 2016

## 1. Introduction

Recent research in the field of batteries has moved from focusing on lithium (Li) air or ion batteries to air batteries that use highly abundant metals due to the cost-effectiveness, the benign issue of obtaining anodes, and cell stability.<sup>1</sup> It is well known that Li metal is very expensive,<sup>2</sup> and there are safety concerns because Li is flammable. Thus, several metals such as zinc, aluminum, and magnesium have been investigated as battery anodes to overcome these issues.<sup>3-11</sup> Aluminum is a great candidate for metal-air batteries owing to its high capacity and energy density, abundance, and sustainability. The theoretical energy density of aluminum is 4300 Wh/g, which is second only to that of lithium (5200 Wh/g).<sup>12,13</sup> Due to the high potential of these properties, Al air batteries have been considered a potential energy source for electric vehicles.<sup>14,15</sup>

Further, surface modifications of Al anodes have also been studied to improve battery performance and stability. For example, Al alloys with gallium, lead, zinc, magnesium, and tin were prepared to reduce

surface corrosion rate.<sup>16,17</sup> Metal oxide layers were coated on the surface of Al anodes to prevent surface oxidation during cell performance.<sup>16,18,19</sup> However, in these cases, it is hard to release Al ions from the Al surface due to a thick surface barrier. In addition, inserted metal species in the alloy case could be unexpectedly released during cell operation. Consequently, by-products could be generated during battery operation, and these by-products could negatively affect battery performance.

In this study, to overcome such bottlenecks and improve battery performance, a physically modified Al anode based air battery was manufactured. In this case, off-the-shelf Al foil was used as the battery anode and was sandblasted using 10  $\mu\text{m}$  metal oxide beads to increase the surface area and reactivity.<sup>20</sup> Al electrode surface morphologies and lattices were characterized according to treatment and the electrochemical properties of the manufactured Al air battery was also analyzed. As expected, the discharging performance and specific energy density were improved in the sandblasted Al anode compared with the bare Al surface. In addition, an electrolyte solution was

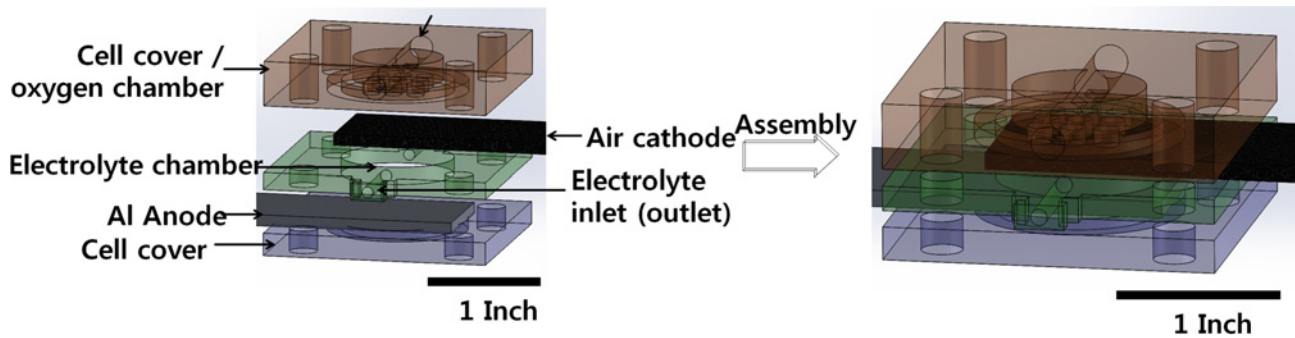


Fig. 1 Assembly diagram of Al air battery, not to scale

circulated between the battery structures for cell stability and enhanced battery performance. The improved performance is a result of the fact that by-products from the Al anode reaction during cell operation could be removed from the electrolyte and fresh electrolyte could be fed by electrolyte circulation.

## 2. Experimental

### 2.1 Materials and Instruments

Off-the shelf Al foil (ALCAN™) was used as an anode. A carbon-based E-4A Air cathode was purchased from Electric Fuel. Sodium hydroxide, ammonium chloride, and aluminum chloride were purchased from Sigma Aldrich. The surface of the Al was physically modified by a sandblaster (Basic classic, Renfert GmbH, Germany). The electrolyte solution was circulated through a peristaltic pump (VWR pump variable flow, VWR international, Canada). The sandblasted Al anode was depicted by SEM (XL30, FEI, USA). The surface roughness was measured by optical surface profiler (ZeScope optical profiler, omniscan, UK). The battery performance was demonstrated by potentiostat/galvanostat (SP-150, BioLogic, France)

### 2.2 Design of Al Air Battery and Manufacturing

First, 10 micron metal oxide beads were bombarded on the Al surface for 5 minutes to prepare the sandblasted Al anode, after which nickel mesh was connected to the Al surface for charge collection. For the electrolyte, a 0.5 M solution of sodium hydroxide, ammonium chloride, and aluminum chloride was mixed and injected into the electrolyte chamber. The battery structure parts were manufactured by a 3D printer; the parts had tubing inserts to supply the electrolyte (Fig. 1).

### 2.3 Cell Performance Test

Based on the design of the cell structure, cyclic-voltammetry (CV) was measured using a bare Al anode and a sandblasted Al anode with a scanning rate of 20 mV/s. The starting potential was 0 V and was swept between -2.0 V to 2.0 V for 3 cycles. In addition, discharging properties were measured for each anode (with and without sandblasting, and with and without the electrolyte circulation process) by potentiostat/galvanostat system at 1 mA. An LED light (working potential: -1.6 V) was turned on by the assembled Al air battery. The electrolyte was injected into a chamber through an inlet by a peristaltic pump and flowed out via an outlet. In that case, flow rate for electrolyte

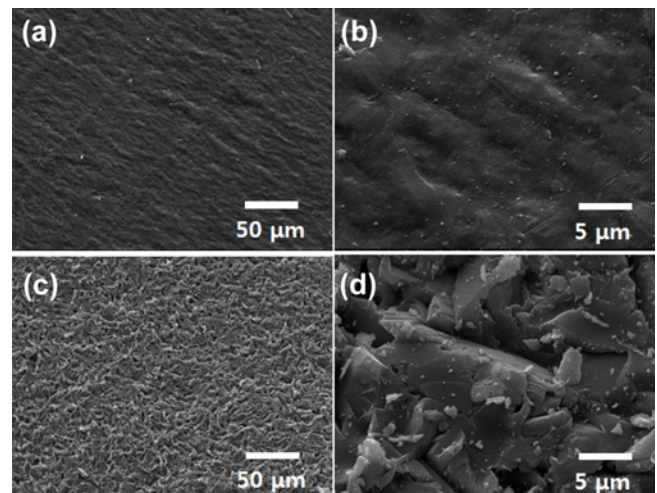


Fig. 2 SEM images of (a) 1 k x, (b) 10 k x bare Al anode structure and (c) 1 k x, (d) 10 k x sandblasted Al anode structure

circulation was 0.8 mL/min. In addition, oxygen flowed into the cathode cell cover to increase the cathode reaction.

## 3. Results and Discussion

The Al air battery structure is illustrated in Fig. 1. The electrolyte outlet of one battery could be connected with the inlet of another battery, allowing the electrolyte to flow continuously through several batteries. As a result, several cells could be connected in series using one electrolyte solution, and the cell potential could very simply be increased. The gas inlet was installed on the lateral face of the top cover layer to increase the air cathode reactivity with oxygen.

The morphologies of the Al anodes were observed by SEM according to surface treatment. Figs. 2(a) and 2(b) show smooth and clean Al surfaces. After the sandblasting process, SEM images capture rough surfaces of the Al foil as shown in Figs. 2(c) and 2(d). This increased surface area was created to enhance reactivity, and the aluminum oxide layer of the Al foil top layer could be removed by the sandblasting process. Also, pores were observed on the surface of the Al; it could be estimated that the Al oxidation reaction could occur on the surface and also inside the Al anode during cell operation. In addition, the surface roughness of the sandblasted Al anode was measured by optical surface profiler, and as a result, its roughness was 2.2957  $\mu\text{m}$ . Thus, the sandblasting process improved the active area of

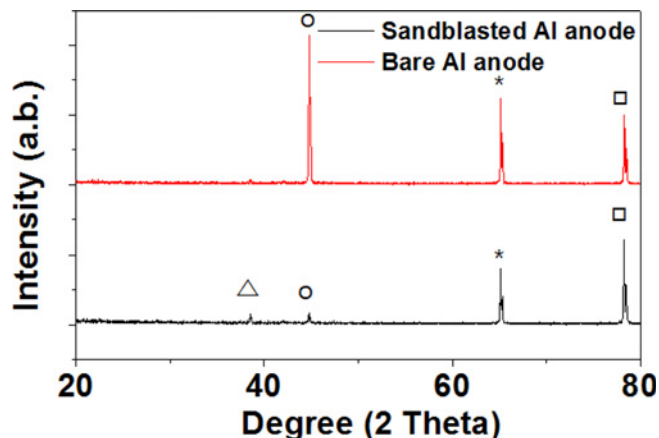


Fig. 3 XRD patterns of Al anodes

the Al anode. After the sandblasting process at ambient conditions, the Al surface activity increased due to the strong impact of the sand, and as a result, a surface oxidation process was induced by the oxygen in the air. However, this Al oxide layer could protect against damage caused by sodium hydroxide and prevent vigorous surface reactions. Thus, surface stability could be improved by the sandblasting process.

Fig. 3 depicts XRD patterns of the Al electrode.<sup>21</sup> Before sand blasting, a diffraction pattern (o, hkl; 400) at around 45 degrees was clearly observed, however, after surface treatment, this pattern was dramatically reduced. This indicated that the aluminum oxide peak was reduced by the sand blasting process. This means that the thickness of the aluminum oxide layer was decreased, and as a result, it was expected that Al ions could be more easily released from the sandblasted Al anode.

In addition, a new diffraction pattern (△, hkl; 311) at around 37 degrees appeared after sand blasting. This indicates that a new, thin aluminum oxide layer was formed due to Al surface activation after the sandblasting impact. Around 65 (\*, hkl; 220) and 78 (□, hkl; 311) degrees, two diffraction patterns were measured and were oriented through the Al lattice. In this case, the intensity of Al diffraction was reduced at 65 degrees, which may be correlated with the reduction of the amount of aluminum in the aluminum oxide (400) layer.

The CV properties of the Al air battery were measured for both surface conditions of the Al anode. In the smooth Al anode case, the oxidation peaks were shrunk via repeating cycles (Fig. 4(a), over 1.66 V). However, the peaks in the sandblasted Al anode were reversible and overlapped during measurement as shown in Fig. 4(b). Therefore, the sandblasted Al anode was more stable than the smooth anode. In addition, the CV curve area of the sandblasted cell was larger than that of the smooth case. This means that the capacitance of the sandblasted anode-based battery was higher than that of the smooth anode-based battery.<sup>22</sup> The oxidation peak of both Al anodes were measured to be approximately 1.6 V (Al → Al<sup>3+</sup> + 3e<sup>-</sup>; 1.66 V).

In Fig. 5(a), discharging curves are depicted according to the anode condition. In the case of the sandblasted anode, the initial potential was 0.8 V, and it was exhausted after 5.5 hrs. In contrast, the bare Al anode initially generated 0.8 V, and was exhausted after 1 hr. As expected, the battery discharging period for the surface treated anode-based cell was longer than the smooth Al anode-based cell. These results correspond well

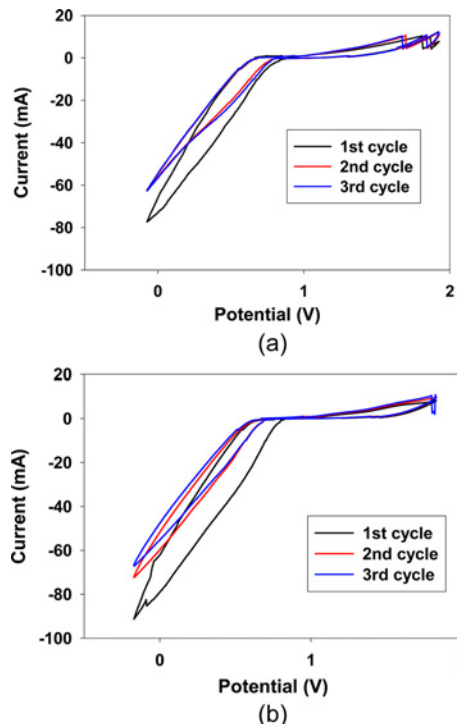


Fig. 4 CV curves according to anode conditions: (a) Smooth Al anode, (b) Sandblasted Al anode for 3 cycles

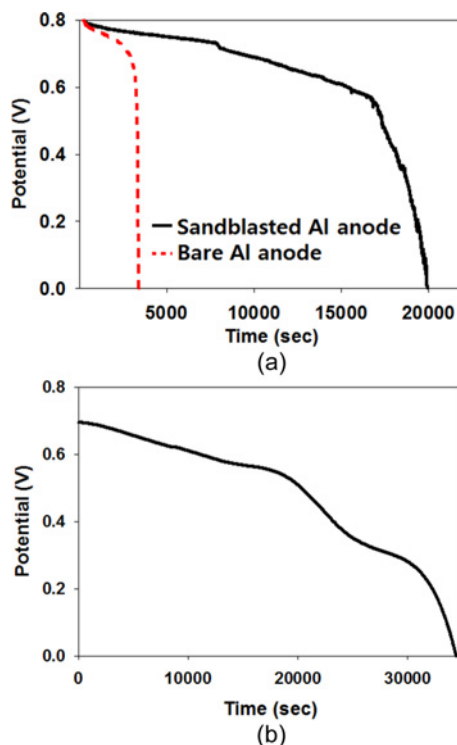


Fig. 5 Discharging curves depending on (a) Anode conditions, (b) The electrolyte circulating process at 1 mA/cm<sup>2</sup>

with the CV curve data.<sup>19</sup> The sandblasted Al showed more uniform dissolution during discharging while the smooth Al barely dissolved, and was electrically disconnected. This result implies that the rough surface induces uniform dissolution to maintain electrical contact. Furthermore, discharging curves were measured depending on the electrolyte

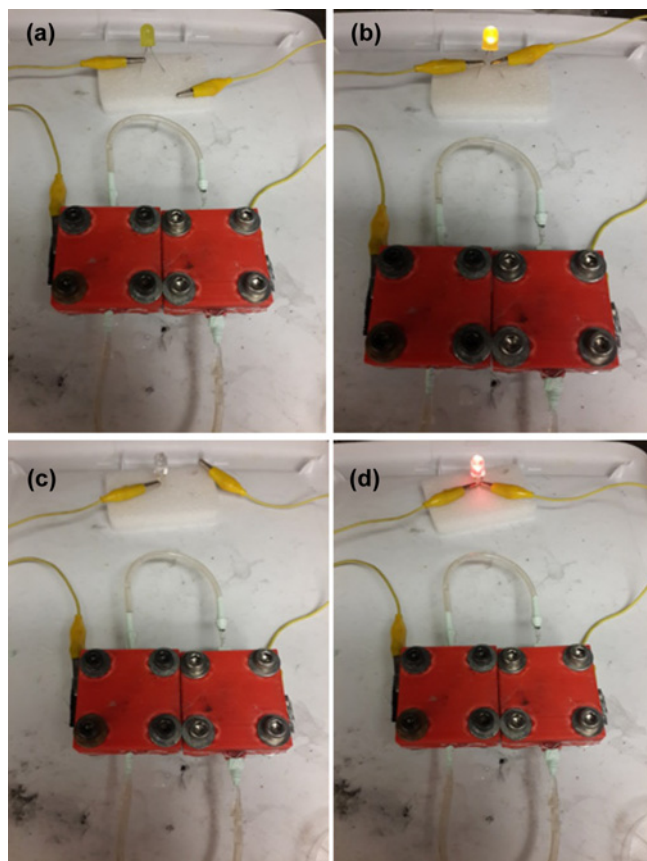


Fig. 6 LED performance test with multi cells: (a) and (c) Cells were disconnected, (b) and (d) were connected with LED

circulation as shown in Fig. 5(b). The discharging period in the circulation was about 10 hrs. The discharging rate in the case with circulation was slower compared to the case without electrolyte circulation.

After a certain operation time, Al ion concentration increased in the electrolyte solution without circulation, and by-products were generated during cell performance. However, for the electrolyte circulation process, the accumulation of Al ions in the electrolyte could be prevented. Thus, at the point of chemical dynamic equilibrium, Al ions could be continuously released from the Al anode. As a result, cell performance was improved using electrolyte circulation. Furthermore, the chance of by-product formation could be reduced by this process. The results showed an energy capacity of 0.7 mWh in the bare Al anode case, but 3.85 mWh in the sandblasted Al anode case. Therefore, the sandblasting process improved the energy capacity by a factor of 5.5. In addition, the energy capacity in the electrolyte circulation case was 4.5 mWh at 1 mA/cm<sup>2</sup>, and it was established that performance was enhanced approximately 6.5 times by the sandblasting and electrolyte circulation process. Other researchers have reported the energy capacity of Al batteries depending on the Al anode conditions. In the case of ceramic protected Al anodes, energy capacity was 1.3 mWh at 1 mA/cm<sup>2</sup>,<sup>19</sup> while metal alloyed Al anodes gave an energy capacity of 4.16 mWh at 0.8 mA/cm<sup>2</sup>.<sup>17</sup> Thus, the sandblasted Al anode and electrolyte circulation based battery structure might possess potential for energy applications.

LED light tests were carried out to visualize the Al air battery's performance. Using two batteries, the red and yellow lights of the LED

lamps (working voltage -1.6 V) were lit as shown in Figs. 6(b) and 6(d). The potential of a single cell was -0.8 V and, therefore, two batteries were connected in series for the lighting test as the required working voltage was 1.6 V.

#### 4. Conclusions

The surface of an Al anode was physically modified by a sandblasting process to improve battery performance. After the sandblasting process, the surface area and active site of the Al anode was dramatically increased, and suitable oxygen content helped to form an oxide layer, which offered anode stability. According to the CV and discharging performance, the sandblasted Al anode-based battery properties increased in performance by 5.5 times compared to the bare Al anode battery case. In addition, electrolyte circulation was used to further enhance the performance of the Al air battery. As a result, cell potential improved 6.5 times compared to the case without circulation. In addition, an LED light test was successfully demonstrated by using two batteries connected in series. Therefore, physically altering the surface and using electrolyte circulation can enhance Al battery performance. However, in this study, a sandblasted Al anode was used for a primary air battery. Thus, to achieve a better performance and application, a sandblasted Al anode should be modified for use in a secondary Al air battery.

#### ACKNOWLEDGEMENTS

The authors would like to acknowledge the support of the Natural Sciences and Engineering Research Council of Canada (NSERC), Alberta Innovates Technology Future (AITF). This research was also supported by the Calgary Advanced Energy Storage and Conversion Research (CAESR) in the University of Calgary and an Eyes High research fellowship from the University of Calgary.

#### REFERENCES

1. Wang, H., Bai, Y., Chen, S., Luo, X., Wu, C., et al., "Binder-Free V<sub>2</sub>O<sub>5</sub> Cathode for Greener Rechargeable Aluminum Battery," ACS Applied Materials & Interfaces, Vol. 7, No. 1, pp. 80-84, 2014.
2. Petri, R., Giebel, T., Zhang, B., Schünemann, J.-H., and Herrmann, C., "Material Cost Model for Innovative Li-Ion Battery Cells in Electric Vehicle Applications," Int. J. Precis. Eng. Manuf.-Green Tech., Vol. 2, No. 3, pp. 263-268, 2015.
3. Lin, M.-C., Gong, M., Lu, B., Wu, Y., Wang, D.-Y., et al., "An Ultrafast Rechargeable Aluminium-Ion Battery," Nature, Vol. 520, No. 7547, pp. 324-328, 2015.
4. Li, Y., Gong, M., Liang, Y., Feng, J., Kim, J.-E., et al., "Advanced Zinc-Air Batteries Based on High-Performance Hybrid Electrocatalysts," Nature Communications, Vol. 4, Paper No. 1805, 2013.

5. Jayaprakash, N., Das, S. K., and Archer, L. A., "The Rechargeable Aluminum-Ion Battery," *Chemical Communications*, Vol. 47, pp. 12610-12612, 2011.
6. He, Y. J., Peng, J. F., Chu, W., Li, Y. Z., and Tong, D. G., "Black Mesoporous Anatase TiO<sub>2</sub> Nanoleaves: A High Capacity and High Rate Anode for Aqueous Al-ion Batteries," *Journal of Materials Chemistry A*, Vol. 2, No. 6, pp. 1721-1731, 2014.
7. Prabu, M., Ramakrishnan, P., Nara, H., Momma, T., Osaka, T., et al., "Zinc-Air Battery: Understanding the Structure and Morphology Changes of Graphene-Supported CoMn<sub>2</sub>O<sub>4</sub> Bifunctional Catalysts under Practical Rechargeable Conditions," *ACS Applied Materials & Interfaces*, Vol. 6, No. 19, pp. 16545-16555, 2014.
8. Hiralal, P., Imaizumi, S., Unalan, H. E., Matsumoto, H., Minagawa, M., et al., "Nanomaterial-Enhanced All-Solid Flexible Zinc-Carbon Batteries," *ACS Nano*, Vol. 4, No. 5, pp. 2730-2734, 2010.
9. Sun, X., Duffort, V., Mehdi, B. L., Browning, N. D., and Nazar, L. F., "Investigation of the Mechanism of Mg Insertion in Birnessite in Nonaqueous and Aqueous Rechargeable Mg-Ion Batteries," *Chemistry of Materials*, Vol. 28, No. 2, pp. 534-542, 2016.
10. Ha, S. Y., Lee, Y. W., Woo, S. W., Koo, B., Kim, J. S., et al., "Magnesium (II) Bis (Trifluoromethane Sulfonyl) Imide-Based Electrolytes with Wide Electrochemical Windows for Rechargeable Magnesium Batteries," *ACS Applied Materials & Interfaces*, Vol. 6, No. 6, pp. 4063-4073, 2014.
11. Jia, X., Yang, Y., Wang, C., Zhao, C., Vijayaraghavan, R., et al., "Biocompatible Ionic Liquid-Biopolymer Electrolyte-Enabled Thin and Compact Magnesium-Air Batteries," *ACS Applied Materials & Interfaces*, Vol. 6, No. 23, pp. 21110-21117, 2014.
12. Fan, L., Lu, H., Leng, J., Sun, Z., and Chen, C., "The Effect of Crystal Orientation on the Aluminum Anodes of the Aluminum-Air Batteries in Alkaline Electrolytes," *Journal of Power Sources*, Vol. 299, pp. 66-69, 2015.
13. Hibino, T., Kobayashi, K., and Nagao, M., "An All-Solid-State Rechargeable Aluminum-Air Battery with a Hydroxide Ion-Conducting Sb(V)-Doped SnP<sub>2</sub>O<sub>7</sub> Electrolytes," *Journal of Materials Chemistry A*, Vol. 1, No. 47, pp. 14844-14848, 2013.
14. Zhang, X., Yang, S. H., and Knickle, H., "Novel Operation and Control of an Electric Vehicle Aluminum/Air Battery System," *Journal of Power Sources*, Vol. 128, No. 2, pp. 331-342, 2004.
15. Yang, S. and Knickle, H., "Design and Analysis of Aluminum/Air Battery System for Electric Vehicles," *Journal of Power Sources*, Vol. 112, No. 1, pp. 162-173, 2002.
16. Egan, D., De León, C. P., Wood, R., Jones, R., Stokes, K., et al., "Developments in Electrode Materials and Electrolytes for Aluminium-Air Batteries," *Journal of Power Sources*, Vol. 236, pp. 293-310, 2013.
17. Pino, M., Chacón, J., Fatás, E., and Ocón, P., "Performance of Commercial Aluminium Alloys as Anodes in Gelled Electrolyte Aluminium-Air Batteries," *Journal of Power Sources*, Vol. 299, pp. 195-201, 2015.
18. Mori, R., "A Novel Aluminium-Air Rechargeable Battery with Al<sub>2</sub>O<sub>3</sub> as the Buffer to Suppress Byproduct Accumulation Directly onto an Aluminium Anode and Air Cathode," *RSC Advances*, Vol. 4, No. 57, pp. 30346-30351, 2014.
19. Mori, R., "Addition of Ceramic Barriers to Aluminum-Air Batteries to Suppress by-Product Formation on Electrodes," *Journal of the Electrochemical Society*, Vol. 162, No. 3, pp. A288-A294, 2015.
20. Bok, W.-M., Kim, S.-Y., Lee, S.-J., Shin, G.-S., Park, J.-M., et al., "Surface Characteristics and Bioactivation of Sandblasted and Acid-Etched (SLA) Ti-10Nb-10Ta Alloy for Dental Implant," *Int. J. Precis. Eng. Manuf.*, Vol. 16, No. 10, pp. 2185-2192, 2015.
21. Samantilleke, A., Carneiro, J., Azevedo, S., Thuy, T., and Teixeira, V., "Electrochemical Anodizing, Structural and Mechanical Characterization of Nanoporous Alumina Templates," *Journal of Nano Research*, Vol. 25, pp. 77-89, 2013.
22. Chen, W., Fan, Z., Gu, L., Bao, X., and Wang, C., "Enhanced Capacitance of Manganese Oxide via Confinement inside Carbon Nanotubes," *Chemical Communications*, Vol. 46, No. 22, pp. 3905-3907, 2010.